A&A 537, A27 (2012)
DOI: 10.1051/0004-6361/201117197

Astronomy & Astrophysics

The deep 3.4 μm interstellar absorption feature toward the IRAS 18511+0146 cluster

M. Godard[1], T. R. Geballe[2], E. Dartois[1], and G. M. Muñoz Caro[3]

[1] Institut d'Astrophysique Spatiale (IAS, UMR 8617), CNRS; Université Paris-Sud, Bât. 121, 91405 Orsay, France
e-mail: marie.godard@ias.u-psud.fr
[2] Gemini Observatory, 670 N. A'ohoku Place, Hilo, HI 96720, USA
[3] Centro de Astrobiología (CSIC-INTA), Ctra. de Ajalvir, km 4, Torrejón de Ardoz, 28850 Madrid, Spain

Received 6 May 2011 / Accepted 17 October 2011

ABSTRACT

Context. An absorption feature at 3.4 μm, widely observed in the diffuse interstellar medium (ISM), is produced by aliphatic hydrocarbon dust. In the local ISM there is in general a linear correlation between the 3.4 μm optical depth and the visual extinction A_V. However, the 3.4 μm optical depth toward the young stellar object IRAS 18511+0146, the highest found in the local diffuse ISM apart from the Galactic centre lines of sight, is three times higher than predicted from the most likely value for the distance of the object, the extinction-distance relation for the Galactic diffuse ISM, and the value of $A_V/\tau_{3.4}$ in the Galactic disk.
Aims. IRAS 18511+0146 is associated with a small cluster of stars. We have obtained spectra of it as well as two other cluster members in order to verify the unusually high 3.4 μm optical depth toward IRAS 18511+0146 and test for patchiness in the foreground diffuse cloud material.
Methods. Spectra covering 2.9–4.1 μm were recorded using the near-infrared imager/spectrograph (NIRI) at the Gemini North telescope.
Results. After subtraction of the superimposed 3.47 μm band, produced in dense interstellar gas associated with the cluster, we have determined optical depths of 0.06–0.08 for the 3.4 μm absorption on the three lines of sight. We discuss the distance and extinction to the IRAS 18511+0146 cluster and possible interpretations of the high optical depth of the 3.4 μm absorption.
Conclusions. The most probable distance to the IRAS 18511+0146 cluster is 3.9 kpc. Two different interpretations of the high observed $\tau_{3.4}$ are then possible. (i) The A_V to distance ratio toward the cluster is approximately the one observed on average in the Galactic diffuse ISM, in which case $A_V \sim 7$ and $\tau_{3.4}$ in this direction is three times higher than predicted by the usual $A_V/\tau_{3.4}$ observed in local diffuse ISM. (ii) The visual extinction in the direction of the IRAS 18511+0146 cluster is higher (i.e. 15–20 mag), probably due to a diffuse cloud associated with the cluster, resulting in a high value of $\tau_{3.4}$. In either case, the high $\tau_{3.4}$ makes this cluster a unique and valuable line of sight for studying the Galactic hydrocarbon dust.

Key words. methods: observational – techniques: spectroscopic – infrared: ISM – ISM: lines and bands – dust, extinction – stars: individual: IRAS 18511+0146

1. Introduction

An infrared absorption feature at 3.4 μm is widely observed in the diffuse interstellar medium (ISM) and constitutes a major IR signature of carbonaceous interstellar dust. The feature is produced by C-H stretching vibrations in the methyl (-CH_3) and methylene (-CH_2-) groups of hydrocarbons. It was first detected in lines of sight toward the Galactic centre (GC) (Soifer et al. 1976; Wickramasinghe & Allen 1980; McFadzean et al. 1989) and then in other sight lines in the Milky Way (e.g. Adamson et al. 1990; Sandford et al. 1991; Pendleton et al. 1994) and in other galaxies (e.g. Bridger et al. 1994; Imanishi 2000a,b; Spoon et al. 2004; Dartois & Muñoz-Caro 2007).

A correlation has been found between the 3.4 μm optical depth $\tau_{3.4}$ and the visual extinction A_V as expected for a carrier residing in the diffuse ISM. However, Sandford et al. (1991) noticed that this increase is not linear over the entire A_V range, but rises significantly at the highest A_V values (≈30−35), which are all associated with sources in the Galactic centre. The difference between Galactic centre sources and those on other sight lines was confirmed by Pendleton et al. (1994) who also observed additional sources and extended the study of $\tau_{3.4}$ vs. A_V to lower A_V. They found a ratio $A_V/\tau_{3.4} \approx 150$ toward the Galactic centre and $A_V/\tau_{3.4} \approx 250$ for other directions. Similar results were later obtained by Imanishi et al. (1996) and Rawlings et al. (2003). Sandford et al. (1995) concluded from this behaviour that the grains responsible for the diffuse ISM aliphatic C-H bands are different from those responsible for much of the observed visual extinction in the diffuse ISM. They also interpreted it as resulting from a non-uniform distribution of the aliphatic hydrocarbon component of the diffuse ISM throughout the Galaxy (i.e. an increase of its abundance in the inner part of the Galaxy[1]).

The strongest reported 3.4 μm absorption feature outside the Galactic centre region is on the line of sight to the young stellar object IRAS 18511+0146 (Ishii et al. 1998). An $R \sim 1400$ spectrum of this band was obtained by Ishii et al. (2002). The 3.4 μm absorption feature lies on the long-wavelength edge of the 3.1 μm water ice band absorption. The water-ice band does not arise in the diffuse ISM, but is present in the molecular cloud in which IRAS 18511+0146 is embedded.

[1] This could also be interpreted as a decrease of the non-aliphatic extinction-producing material in the central regions of the Galaxy.

Table 1. Log of the spectroscopic observations.

Source	Observation date	Exposure time	Standard star			
		(s)	Name	Spectral type	$T_{\rm eff}$ (K)	L-band magnitude
S7	12 March 2009	240	HIP 89601	F2V	6980[a]	5.80
S10	19 May 2009	2880	HIP 95253	F6V	6340[b]	5.15
S11	7 May 2009	7200	HIP 89601	F2V	6980[a]	5.80

Notes. [(a)] Boesgaard & Tripicco (1986); [(b)] Balachandran (1990).

Table 2. Observed sources.

Source	Position (J2000)		Palomar magnitude			*Spitzer*-IRAC magnitude			
	α	δ	J	H	$K_{\rm S}$	3.6 μm	4.5 μm	5.8 μm	8.0 μm
	(h min s)	($^\circ$ $'$ $''$)	(mag)	(mag)	(mag)	(mag)	(mag)	(mag)	(mag)
S7	18 53 37.9	01 50 30	13.43 ± 0.04	9.30 ± 0.03	6.61 ± 0.03	–	–	–	–
S10	18 53 38.4	01 50 15	–	15.00 ± 0.03	11.11 ± 0.01	7.56 ± 0.08	6.6 ± 0.2	5.65 ± 0.05	4.95 ± 0.07
S11	18 53 38.7	01 50 13	–	17.5 ± 0.2	12.77 ± 0.02	7.61 ± 0.05	6.3 ± 0.2	5.11 ± 0.04	4.32 ± 0.04

Notes. The information is obtained from Table 2 in Vig et al. (2007). Source S7 is IRAS 18511+0146; it is saturated in the IRAC images.

The distance to IRAS 18511+0146 has been listed as 3.9 kpc by Molinari et al. (1996) and Watt & Mundy (1999). Their values are based on the radial velocities of lines observed in the molecular cloud associated with IRAS 18511+0146. The average visual extinction associated with the foreground diffuse ISM may be estimated from the distance of IRAS 18511+0146 and the average ISM extinction vs. distance relation, 1.8 mag kpc^{-1} (Whittet 1992) to be $A_V \sim 7$. If that estimation is correct, the observed optical depth of the 3.4 μm feature is three times higher than predicted by Pendleton et al. (1994) and is well outside the typical scatter in the A_V:$\tau_{3.4}$ correlation. It therefore is of interest to further explore the diffuse ISM probed by this line of sight.

Vig et al. (2007), using multi-wavelength imaging, found that IRAS 18511+0146 is the brightest member of a cluster of stars. Here we report observations of two bright cluster members and IRAS 18511+0146, intended to determine if the apparently anomalously strong 3.4 μm band toward IRAS 18511+0146 is unique to it or is a property of the diffuse ISM in this direction. The observations and data reduction are described in Sect. 2. Results are presented in Sect. 3. The distance to the cluster is discussed in Sect. 4, and a brief discussion follows in Sect. 5.

2. Observations and data reduction

The observations were performed at the Frederick C. Gillett Gemini North telescope on Mauna Kea, using the facility near-infrared imager/spectrograph (NIRI, Hodapp et al. 2003). Spectra covering 2.95–4.15 μm were obtained on UT 2009 March 12, May 7, and May 19 (Gemini program ID: GN-2009A-Q-30). The 0.47$''$ slit provided a resolving power of $R \sim 690$. The sky was photometric on each occasion, although the seeing differed from night to night. More information about the observations is given in Table 1.

Three sight lines in the vicinity of IRAS 18511+0146 (also known as Mol 75 and RAFGL 5542) were observed, S7, S10, and S11 (as designated by Vig et al. (2007); see their Table 2 and Fig. 5). The brightest source, S7, is IRAS 18511+0146 and is the one observed by Ishii et al. (1998) and Ishii et al. (2002). The positions and magnitudes of these sources are given in Table 2.

Spectra of each object and its calibration star (observed at similar airmass either immediately before or immediately after each cluster object) were obtained in the standard stare-nod mode, with 4$''$ nods back and forth along the slit. Resultant frames were flat-fielded and corrected for bad pixels (whose locations were determined from the flat image) by interpolating over the surrounding pixels. Subtracted spectral image frames were generated from nodded pairs and combined to produce the final images. The positive and negative spectra were extracted for both the science targets and their associated standard stars and then combined to produce final raw spectra. Wavelength calibration utilised telluric absorption lines and is accurate to better than 0.001 μm. Correction was made for atmospheric and instrumental transmission by dividing the spectra of cluster objects by those of associated standard stars.

The standard stars were also used to calibrate the flux scale of the science targets. The spectra of targets divided by those of standard stars were multiplied by the spectra of blackbodies, with temperatures $T_{\rm eff}$ corresponding to the individual standard stars (see Table 1), and scaled to their L-band fluxes. The L-band fluxes were derived from the $K - L$ colours of the standard star spectral type (Tokunaga 2000); the K magnitude was obtained from the 2MASS catalog (Cutri et al. 2003). Hydrogen absorption lines in the standard stars were not removed. This results in apparent weak emission features in the final spectra at 3.04 μm (H I Pfϵ), 3.30 μm (H I Pfδ), 3.74 μm (H I Pfγ), and 4.05 μm (H I Brα) (and smaller features at 3.69 μm (H I Hu18), 3.82 μm (H I Hu16), 3.91 μm (H I Hu15), and 4.02 μm (H I Hu14).

3. Results

3.1. Overview of the spectra

The spectra of S7, S10, and S11 are presented in Figs. 1 and 2. The 3.4 μm absorption band is superimposed on the smooth long wavelength wing of the strong 3.1 μm H_2O ice absorption band (see Fig. 1). That wing is represented by the dashed line in Fig. 2 and is the "local continuum" for the 3.4 μm hydrocarbon band and any additional absorption features near it (it is a polynomial of degree 5 fit to all wavelengths outside of the 3.3–3.6 μm region). For each sight line the absorption optical depth relative to the wing of the ice band has been determined by division of the spectrum (solid line) by this continuum. The optical depth spectra are shown in Fig. 3 (black solid lines) and the corresponding maximum optical depths $\tau_{\rm tot}$ are given in Table 3. As explained in Sect. 3.2, $\tau_{\rm tot}$ is the sum of $\tau_{3.4}$ from the hydrocarbon band produced in diffuse ISM and $\tau_{3.47}$, contributed by a broad absorption band observed in dense clouds and centred at 3.47 μm.

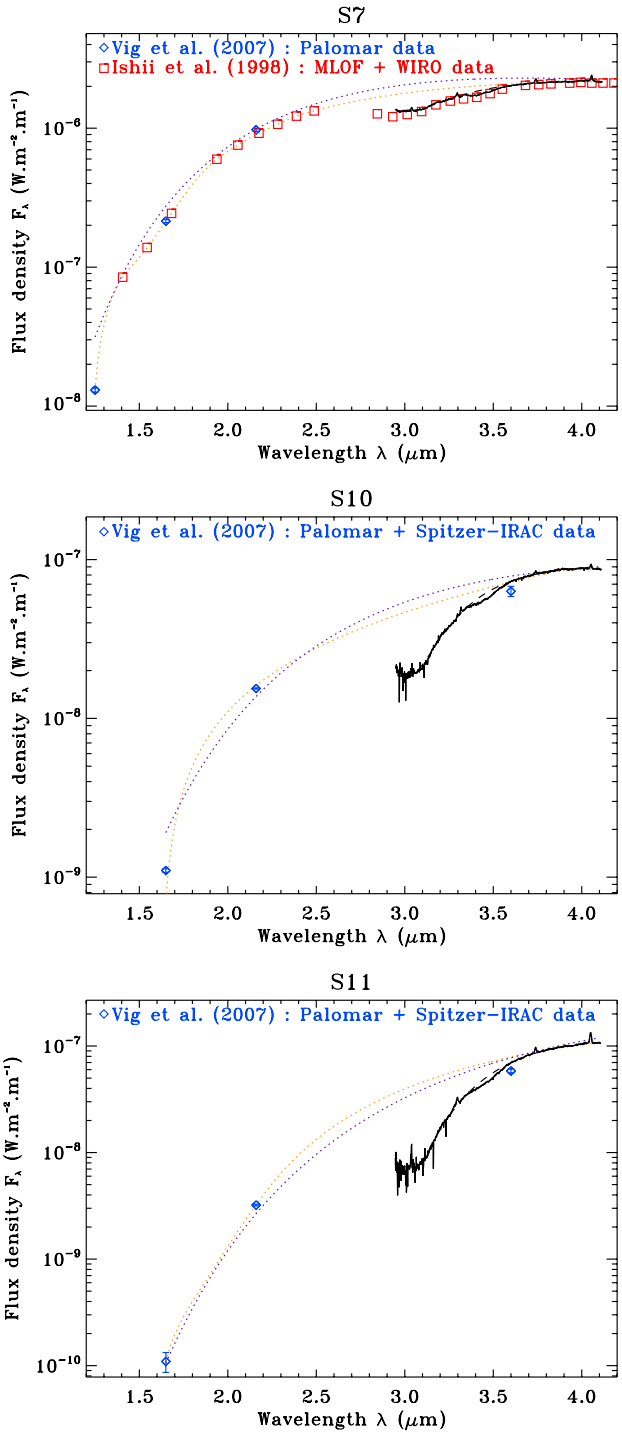

Fig. 1. Spectra of lines of sight toward sources S7, S10, and S11. The blue diamonds and red squares represent the data from Vig et al. (2007) (Palomar and *Spitzer*-IRAC data) and from Ishii et al. (1998) (MLOF and WIRO data), respectively. The dotted lines represent the local continua for the 3.1 μm water ice absorption band. Two different continua are plotted to characterize the uncertainty of the ice band depth: a blackbody function and a spline interpolation are in purple and orange (dark and light grey in the printed version), respectively.

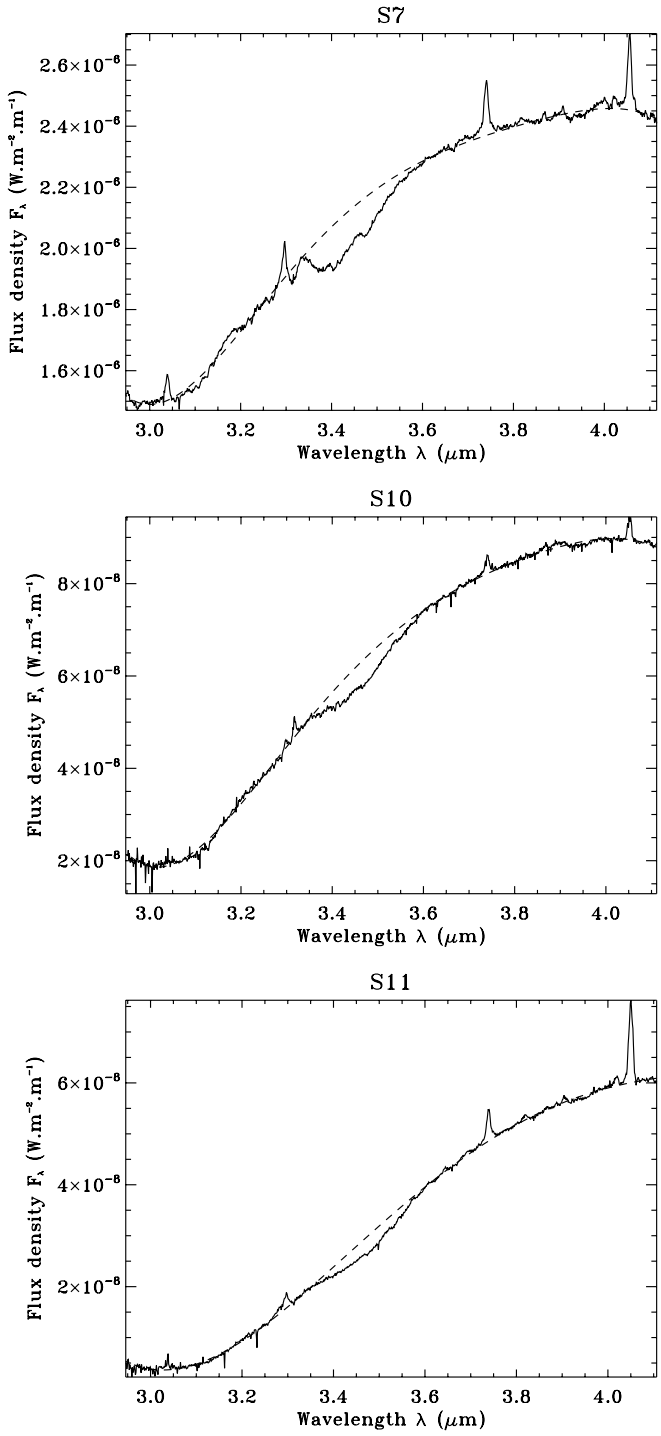

Fig. 2. Spectra of sight lines toward sources S7, S10, and S11, between 2.95 and 4.10 μm. The dashed lines represent the local continua for the 3.4 μm absorption band.

Because the 3.47 μm band and the 3.4 μm band are partially blended on these lines of sight probing both diffuse and dense ISM, it is necessary to subtract the contribution of the 3.47 μm band in order to obtain the profile and maximum optical depth of the 3.4 μm band.

3.2. Removing the contribution of the 3.47 μm band

The 3.47 μm band is a broad (*FWHM* $\sim$ 0.10 μm) and featureless absorption whose shape differs considerably from that of the 3.4 μm hydrocarbon band. Its origin and attribution are

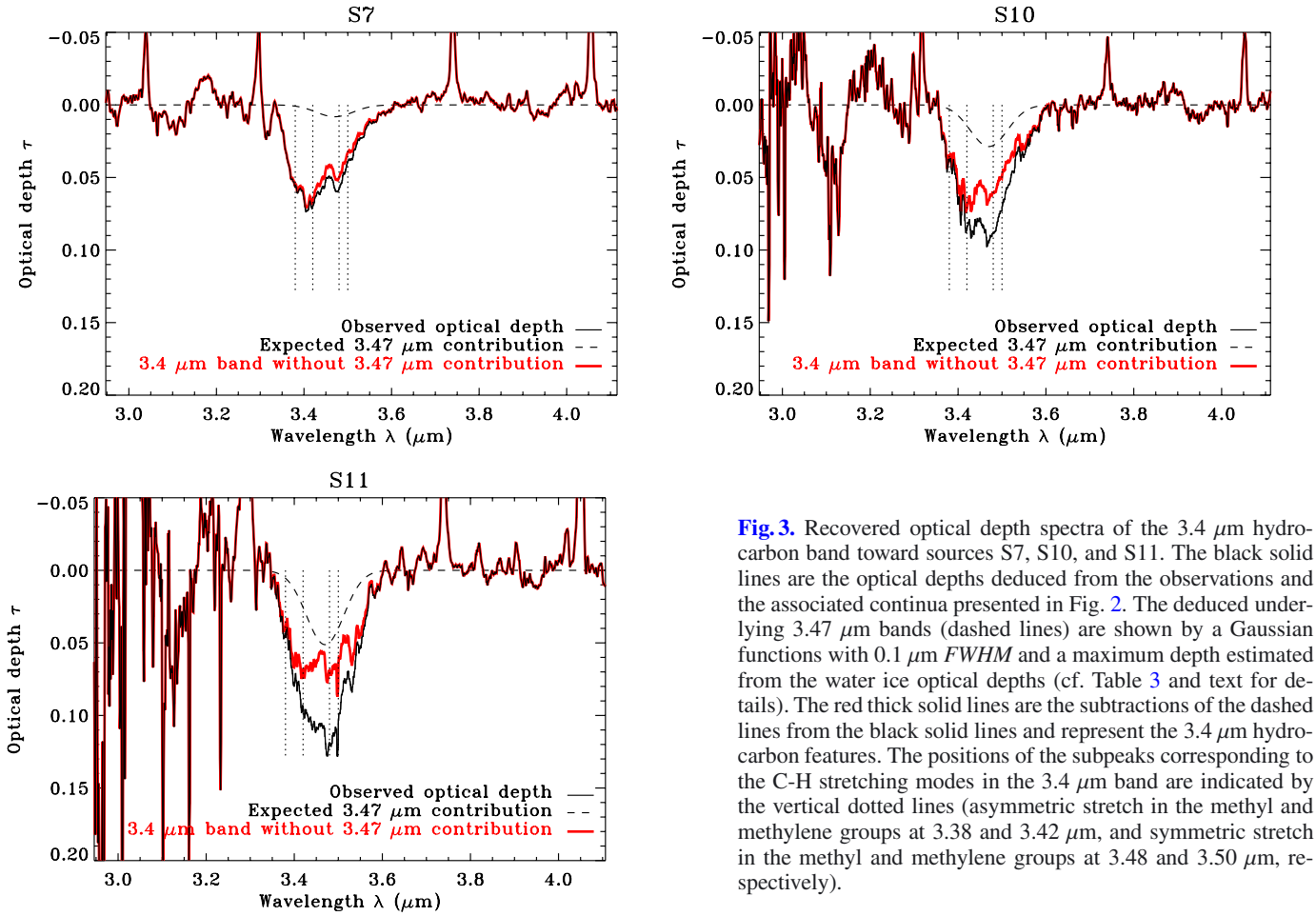

Fig. 3. Recovered optical depth spectra of the 3.4 μm hydrocarbon band toward sources S7, S10, and S11. The black solid lines are the optical depths deduced from the observations and the associated continua presented in Fig. 2. The deduced underlying 3.47 μm bands (dashed lines) are shown by a Gaussian functions with 0.1 μm *FWHM* and a maximum depth estimated from the water ice optical depths (cf. Table 3 and text for details). The red thick solid lines are the subtractions of the dashed lines from the black solid lines and represent the 3.4 μm hydrocarbon features. The positions of the subpeaks corresponding to the C-H stretching modes in the 3.4 μm band are indicated by the vertical dotted lines (asymmetric stretch in the methyl and methylene groups at 3.38 and 3.42 μm, and symmetric stretch in the methyl and methylene groups at 3.48 and 3.50 μm, respectively).

still debated (Allamandola et al. 1993; Chiar et al. 1996; Brooke et al. 1999; Dartois & d'Hendecourt 2001; Dartois et al. 2002; Mennella 2010; Bottinelli et al. 2010). The 3.47 μm optical depth $\tau_{3.47}$ correlates well with the depth of the 3.1 μm water ice band $\tau_{3.1}$. Brooke et al. (1999) found:

$$\tau_{3.47} = (0.033 \pm 0.002)\,\tau_{3.1} - (0.004 \pm 0.004). \quad (1)$$

Thus, in order to correctly remove 3.47 μm bands one must estimate the optical depth of the water ice bands in our spectra. Our data do not include measurements of the continuum on the short wavelength side of the ice band; however, the data of Vig et al. (2007) provide continuum points in the *K* band (they and their uncertainties are shown in Fig. 1). For S7, we also used the data of Ishii et al. (1998). These data and the continua constructed from them are shown in Fig. 1. To evaluate the model-dependent uncertainties in the ice band depth, two different continua were used, as shown in the figure. Our deduced values of $\tau_{3.1}$ and of the corresponding uncertainties are given in Table 3. We then use the Brooke et al. (1999) relation to estimate $\tau_{3.47}$ (cf. Table 3) for each source. In Fig. 3, we represent the estimated underlying 3.47 μm bands (dashed lines) by Gaussian functions with 0.1 μm *FWHM*s. The red solid lines, which are the subtractions of the dashed lines from the black solid lines, contain the pure diffuse ISM 3.4 μm features. The corresponding optical depths are given in Table 3 by $\tau_{3.4} = \tau_{\rm tot} - \tau_{3.47}$.

Note the spectral structure in the pure 3.4 μm band. The subfeatures correspond nicely to the known C-H stretching modes (indicated by the dotted vertical lines in Fig. 3): asymmetric and symmetric stretch in the methyl group (-CH_3) at 3.38 and

Table 3. Optical depths of the different absorption bands for each line of sight.

Source	$\tau_{3.1}$	$\tau_{3.47}$ (Eq. (1))	$\tau_{\rm tot}$	$\tau_{3.4}$ ($=\tau_{\rm tot} - \tau_{3.47}$)
S7	0.36 ± 0.08	0.008 ± 0.007	0.073 ± 0.005	0.065 ± 0.012
S10	1.00 ± 0.08	0.029 ± 0.009	0.093 ± 0.008	0.064 ± 0.017
S11	1.60 ± 0.02	0.049 ± 0.010	0.119 ± 0.012	0.070 ± 0.020

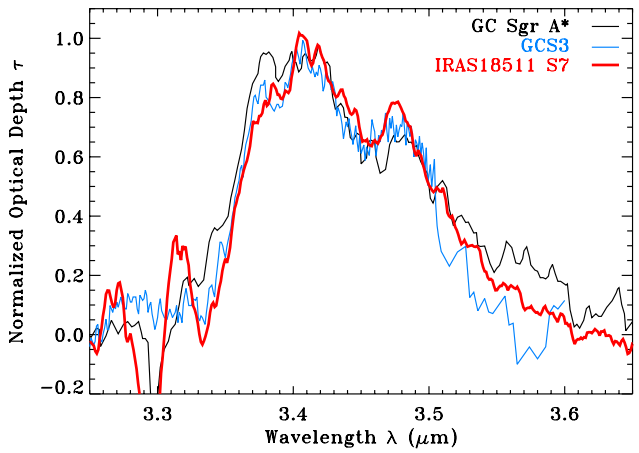

Fig. 4. Comparison of the 3.4 μm band profile observed toward IRAS 18511+0146 (S7, thick red line) and Galactic centre sources, Sgr A* (thin black line) and GCS3 (thin blue line) (from Chiar et al. 2000).

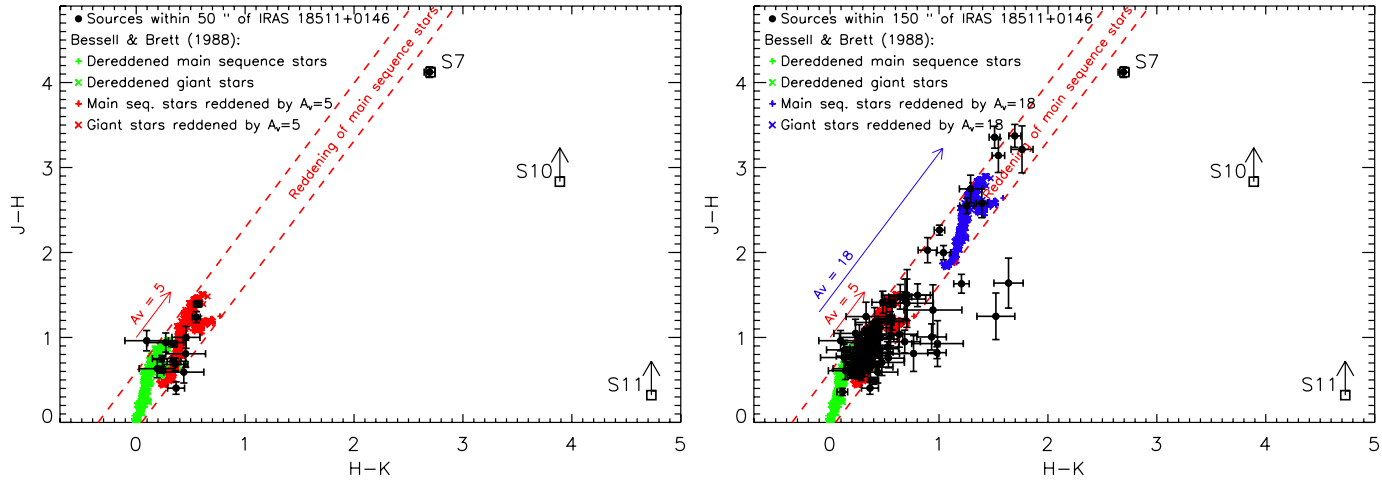

Fig. 5. *(Left)* $(J-H)$–$(H-K)$ colour–colour diagram of sources within 50″ of IRAS 18511+0146 (black dots). These sources and the associated JHK_S magnitudes are found in the 2MASS All-Sky Point Source Catalogue. The red dashed lines delimit the reddening band of main sequence stars. The effect of an interstellar extinction of $A_V = 5$ is indicated by the red arrow (Rieke & Lebofsky 1985). The loci of main sequence and giant branch dereddened stars are represented by the green crosses (Bessell & Brett 1988) and the corresponding stars reddened by $A_V = 5$ are the red crosses. *(Right)* Same as the left diagram, but with sources lying within a radius of 150″ of IRAS 18511+0146. A visual extinction vector of $A_V = 18$ and the corresponding reddened main sequence stars are represented in blue. The positions of S7, S10, and S11 in this diagram are indicated, but for S10 and S11 only lower limits are given because of the non-detection of these source in the J band (cf. Table 2).

3.48 μm, and asymmetric and symmetric stretch in the methylene group (-CH_2-) at 3.42 and 3.50 μm, respectively. In Fig. 4, the 3.4 μm band profile observed toward S7 is compared to those seen in direction of the Galactic centre. This detailed agreement, not only in wavelength, but also in prominence of the substructure compared to purely diffuse sightlines, confirms that the extracted 3.4 μm band is largely due to hydrocarbons and that any under- or over-correction for the 3.47 μm band (which has no substructure) is small.

From the foregoing we conclude that the 3.4 μm band optical depth is similar in all three cluster sources and unusually strong in view of the apparent distance to the cluster.

4. The distance to IRAS 18511+0146

To properly interpret the strengths of the observed 3.4 μm absorption bands, it is critical to be certain of the distance to the IRAS 18511+0146 cluster. In this section we estimate the distance using a number of techniques.

4.1. Distances derived from Galactic rotation

Distances to objects in the Galactic disk can be estimated assuming that the observed radial velocities of the sources arise from Galactic rotation[2] (e.g. Brand & Blitz 1993). For sources located in the inner Galaxy, such as IRAS 18511+0146 two values of kinematic distance from the Sun are possible. For IRAS 18511+0146, the near distance, 3.9 kpc, corresponds to the first intersection of the line of sight with the Sagittarius arm of the Galaxy. This is the distance conservatively assumed by Molinari et al. (1996). However, due to the low galactic latitude of the source, the distance from the Galactic plane does not allow the far distance to be excluded. The far distance, corresponding to the second intersection with the Sagittarius arm, is 10–10.5 kpc. Note that the far distance, when paired with the Galactic average extinction rate of 1.8 mag/kpc, corresponds to $A_V \sim 18$ mag, and the "normal" Galactic disk value of $A_V/\tau_{3.4}$.

[2] Observed radial velocities are usually assumed to have deviations from pure circular rotation by up to 10 km s^{-1}.

4.2. Distance and extinction derived from colour–colour diagrams

The interstellar extinction to IRAS 18511+0146 can be estimated using the $(J-H)$–$(H-K)$ colour–colour diagrams in Fig. 5. Plotted in the left hand diagram are the sources from the 2MASS All-Sky Point Source Catalogue that are within 50″ of IRAS 18511+0146. We adopt the infrared extinction law given by Rieke & Lebofsky (1985). Increasing reddening due only to interstellar extinction is indicated by the arrows. Main sequence stars should fall between the dashed red lines. The loci of main sequence and giant branch with no reddening are shown by the green crosses (Bessell & Brett 1988) whereas those affected by $A_V = 5$ mag are represented in red. Sources lying to the right of the dashed lines (including the three sources discussed in this article) have local infrared excesses and their foreground extinctions are not so easily determined.

From this diagram, the positions of the main sequence stars allow us to estimate the visual extinction. By comparing the loci of observed sources that are likely main sequence stars (the black dots between red dashed lines) with the loci given by Bessell & Brett (1988) for zero extinction and with the reddening vector, we estimate $A_V = 5 \pm 2$. Given the Galactic disk extinction value of 1.8 mag/kpc, this favours the near distance for the IRAS 18511+0146 cluster.

When the colour–colour diagram is extended to include objects within 150″ of IRAS 18511+0146 (right hand diagram in Fig. 5), sources appear in the main sequence star band reddened by considerably more than 5 mag. A reasonable interpretation is that these stars are located at the far distance discussed earlier. The clump of sources grouped around $A_V \approx 5$ mag is now larger. In this diagram, we have only plotted the sources detected in the J, H and K_S bands, and excluded the sources where there is a lower limit on one of the three bands magnitude (except for S10 and S11). We note, however, that colour–colour diagram

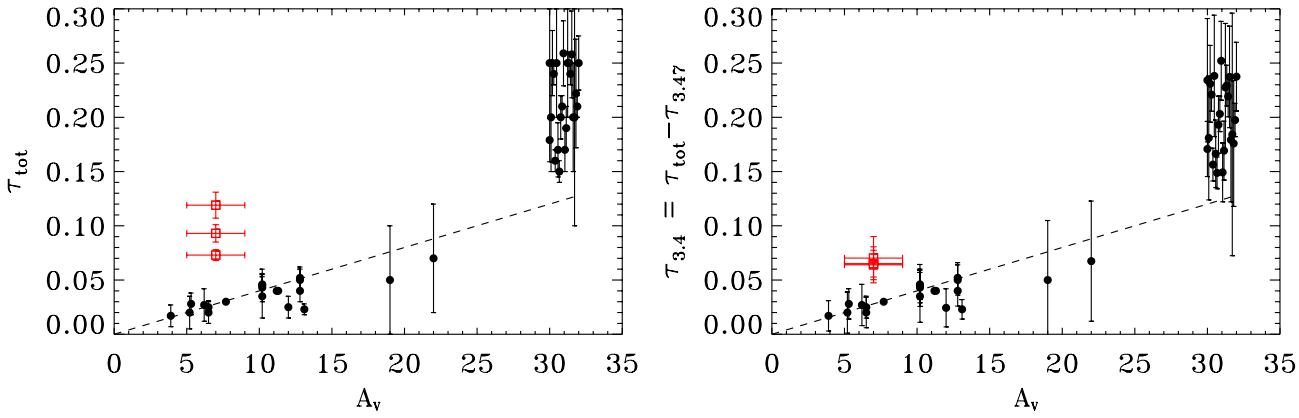

Fig. 6. Optical depth of the C-H stretch band at 3.4 μm vs. visual extinction A_V. The data obtained from this work are shown as red squares. The black filled circles are from McFadzean et al. (1989), Adamson et al. (1990), Sandford et al. (1991), Pendleton et al. (1994), Chiar et al. (2000), Chiar & Tielens (2001), Chiar et al. (2002), Rawlings et al. (2003), and Dartois et al. (2004). The various points associated with the Galactic centre sources have been slightly offset from each other in A_V for clarity (see text for details). *Left*: the optical depths are τ_{tot}; i.e., they include the contribution of the 3.47 μm band. *Right*: the optical depths are $\tau_{3.4}$, due solely to the diffuse ISM (the estimated contributions of the 3.47 μm absorption have been subtracted). In both plots, the dashed line corresponds to the ratio $A_V/\tau = 250$ determined by Pendleton et al. (1994) in the local ISM. See the text for more details about the evaluation of the extinction toward S7, S10, and S11.

for the excluded sources also is consistent with two clumps of main sequence stars corresponding to the near and far distance and extinction-to-distance ratios in this direction close to the 1.8 mag/kpc average.

4.3. Other arguments

Another possible way to address the kinematic distance ambiguity is to search for gas phase atomic or molecular absorption bands toward the IRAS 18511+0146 cluster due to material in front of the cluster. Since the radial velocities of clouds along the line of sight, between the near and far distance points, are greater than the source radial velocity, the local standard of rest (LSR) velocities of absorption features can be used to distinguish between the near and far distance. The H I line at 21 cm and the H_2CO line at 6 cm are often employed for this purpose. Toward IRAS 18511+0146 no absorption with velocity greater than the source v_{LSR} is observed in H_2CO (Araya et al. 2004, 2007). This tends to indicate a near distance for IRAS 18511+0146. However, the far distance cannot be excluded, because of the possible lack of formaldehyde in gas located between the near and far distances.

The detection rates of maser emission, which decrease with increasing source distance, can also provide clues for distinguishing between the near and far distance. Methanol maser emission has been detected in IRAS 18511+0146 at 6.7GHz (class II CH_3OH maser) by Fontani et al. (2010) and Pandian et al. (2007) and at 44 GHz (class I CH_3OH maser) by Kurtz et al. (2004). Fontani et al. (2010) have searched for class I and class II methanol masers in numerous high-mass star-forming. Their detection rates (see their Fig. 3) are ~25% at d = 3–4 kpc, ~10% at d = 8–10 kpc, and none for distance greater than 10 kpc. For the 44 GHz class II maser, the rate is greater than 30% at the near distance and zero at distances greater 8 kpc. These results also suggest the near distance for IRAS 18511+0146, although the possibility of unusually bright maser emission at the far distance cannot be excluded.

The luminosity of the IRAS 18511+0146 sources would be almost one order of magnitude higher if they are at the far distance rather than at the near distance. For the near distance, the luminosity of S7 is estimated at 1–2 $\times$ 10^4 $L_\odot$, and between 10^2 and 10^3 $L_\odot$ for S10 and S11. The far distance would imply that S7, S10 and S11 are equivalent to O- and B-type stars. These luminosities are possible, but the close proximity of several such luminous sources is not frequent.

Finally, the radius of the IRAS 18511+0146 cluster is ~0.6–0.7 pc for a distance of 3.9 kpc (e.g. Vig et al. 2007; Faustini et al. 2009). The far distance would imply a cluster radius of ~1.6–1.8 pc. Faustini et al. (2009) have studied the properties of stellar clusters toward high-mass protostars (including IRAS 18511+0146) and have determined a median cluster radius of 0.7 pc. Only one of the 23 clusters they have detected has a radius between 1.6 and 1.8 pc; all other cluster radii are less than 1.3 pc.

We conclude that, although no individual piece of evidence is completely convincing, the collective weight of all of the evidence is strongly in favour of the near distance of 3.9 kpc for the IRAS 18511+0146 cluster. Although the far distance cannot be firmly excluded, it appears less probable, requiring simultaneously a physically large cluster containing several very luminous objects, low formaldehyde abundance along this sight line between the near and far distance points, unusually powerful methanol maser emissions both at 6.7 and 44 GHz, and the presence of main sequence stars in the near distance foreground, but no main sequence stars detected at the far distance of IRAS 18511+0146.

5. Discussion

In Fig. 6, the optical depth of the 3.4 μm band (with (*left*) and without (*right*) the 3.47 μm band contribution) is shown as a function of the diffuse interstellar extinction A_V for the lines of sight observed by McFadzean et al. (1989), Adamson et al. (1990), Sandford et al. (1991), Pendleton et al. (1994), Chiar et al. (2000), Chiar & Tielens (2001), Chiar et al. (2002), Rawlings et al. (2003), and Dartois et al. (2004). Our estimates for S7, S10, and S11 are shown by red squares; there locations in the plots assume an interstellar visual extinction $A_V \approx 7$

estimated using the most probable distance, 3.9 kpc, and the standard extinction to distance ratio, as discussed earlier. Note in the figure that the values of $\tau_{3.4}$ corresponding to $A_V = 19$ and $A_V = 22$ are particularly uncertain. This is because the spectra from which those values of $\tau_{3.4}$ were determined contain strong photospheric lines of OH near 3.4 μm that blend with the hydrocarbon feature and also because circumstellar dust may also contribute to the extinction (Sandford et al. 1991, 1995).

The interstellar visual extinction toward the Galactic centre is usually assumed to be around 30 mag but is known to vary on small spatial scales over the range $25 \lesssim A_V \lesssim 40$ (e.g. Cotera et al. 2000; Rieke et al. 1989, and references therein). Because of the high extinction, the Galactic centre is unobservable at visible wavelengths and A_V cannot be directly measured. The extinction must thus be determined in the near-infrared and then extrapolated to optical wavelengths using an extinction law to obtain A_V. The extinction to the Galactic centre in the K_S band has been found to be around 3 mag (e.g. Cotera et al. 2000). Schödel et al. (2010) recently determined a mean extinction toward the central parsec of the Galaxy of $A_{Ks} = 2.54$. The most commonly used conversion factor from near-infrared to visual is the ratio $A_V/A_{Ks} \sim 9$ found by Rieke & Lebofsky (1985), but more recent studies toward the GC indicate higher values ($A_V/A_{Ks} \sim 16$, Nishiyama et al. 2008). As remarked by Gosling et al. (2009), this steeper extinction law slope suggests that previous conversions of near-infrared extinction to A_V could have underestimated the values of A_V. Note also that the Galactic centre sightline includes spiral arms and therefore possible dense cloud components that could contribute 10 visual magnitudes (Whittet et al. 1997). Thus, the exact value of A_V arising in the diffuse ISM toward the Galactic centre is difficult to determine, and the relation between A_V and the column density of matter may not be valid as a proxy common to both diffuse ISM and Galactic centre directions. The corresponding data points in Fig. 6 are plotted with $A_V \sim 30$ but their exact positions remain quite uncertain.

In the right hand diagram of Fig. 6, the contribution of the dense ISM $\tau_{3.47}$ has been estimated from $\tau_{\rm ice}$ and subtracted in order to obtain only the diffuse ISM contribution to the absorption. The subtraction has been done not only for the IRAS 18511+0146 sources, but also for those in direction of the Galactic centre, where water ice absorption is also observed. Note that the values of $\tau_{3.4}$ obtained Galactic centre sources are still above the local ISM correlation (the dashed line, i.e. $A_V/\tau = 250$ determined by Pendleton et al. 1994), but the gap between the Galactic centre and local ISM optical depths is significantly smaller when subtracting the 3.47 μm band contribution.

It is clear from Fig. 6 that the optical depths of the 3.4 μm hydrocarbon bands toward the IRAS 18511+0146 cluster sources do not follow the linear correlation with the diffuse interstellar extinction observed in the Galactic disk, if the corresponding extinction is indeed $A_V \approx 7$, but exceed the predicted value by approximately a factor of three. Our understanding of this depends on whether or not the extinction to the young stellar objects in the cluster is the same as that inferred both by the colour-colour diagrams in Fig. 5 for the main sequence stars near the cluster and by the distance combined with the average Galactic A_V to distance value. As underlined by Ishii et al. (2002), interstellar extinction is highly patchy and the A_V to distance ratio can be higher in some particular lines of sight. Moreover, one might expect that remnant diffuse gas would be associated with young clusters and that both their visual extinctions and values of $\tau_{3.4}$ could be higher than predicted from their distances and the average values for Galactic disk extinction vs. distance. For example, toward the young and massive star Cyg OB2 12, which is physically associated with a distinct cloud of diffuse gas, the extinction ratio is 6 ± 1 mag kpc^{-1} (Whittet et al. 1997, and references therein). Values of A_V and $\tau_{3.4}$ would be expected to be more normal for field stars.

For diffuse interstellar gas on the sightline to the IRAS 18511+0146 cluster, an average extinction of 4–5 mag kpc^{-1}, corresponding to a visual extinction of 15–20 mag, would produce the strong 3.4 μm hydrocarbon bands that are observed towards S7, S10, and S11. Further studies of the gas associated with the young cluster are needed to determine if much of the extinction in the diffuse ISM is local to the cluster. Alternatively, observations of stars in front of the IRAS 18511+0146 cluster could determine whether the excess optical extinction and possibly the excess 3.4 μm band strength arise in other locations along the line of sight.

6. Conclusion

We have observed the 3.4 μm absorption band, due to aliphatic C-H stretching modes of interstellar hydrogenated amorphous carbon dust, in three closely spaced lines of sight to young stars in the IRAS 18511+0146 cluster. These observations have confirmed the high optical depth of that band in the diffuse ISM in this direction and have revealed little or no source-to-source variation in it. The 3.4 μm optical depths observed toward these sources are the highest observed in directions other than toward the Galactic centre.

We present several independent observational constraints favouring the previously adopted distance to the cluster of 3.9 kpc, corresponding to the near intersection of the line of sight with the Sagittarius Arm, as opposed to the location of the cluster at far intersection, at a distance of 10–10.5 pc. If the IRAS 18511+0146 cluster is at the far distance, which can still not be firmly excluded but is less probable, this direction would not probe an unusual ISM, but still provide privileged lines of sight to observe high quantities of diffuse ISM dust. Assuming the more probable near distance, the large depth of the 3.4 μm band may be interpreted in two simple ways:

(i) The cluster is associated with a local diffuse cloud that provides excess 3.4 μm optical depth and visual extinction A_V above the amounts predicted by the standard ratio of Galactic distance to A_V, and with the standard Galactic ratio $A_V/\tau_{3.4} \approx 250$ satisfied.
(ii) There is no local diffuse cloud associated with the cluster, and the diffuse ISM probed by this line of sight contains an unusually high abundance of the carrier of the 3.4 μm feature, as shown in Fig. 6.

Further estimates of the distance and the extinction to the IRAS 18511+0146 cluster are needed to properly interpret the high 3.4 μm optical depths. In either case, the high $\tau_{3.4}$ makes this cluster a unique and valuable line of sight for studying Galactic hydrocarbon dust.

Acknowledgements. This paper is based on observations obtained at the Gemini Observatory, which is operated by the Association of Universities for Research in Astronomy, Inc., under a cooperative agreement with the NSF on behalf of the Gemini partnership: the National Science Foundation (United States), the Science and Technology Facilities Council (United Kingdom), the National Research Council (Canada), CONICYT (Chile), the Australian Research Council (Australia), Ministério da Ciência e Tecnologia (Brazil) and Ministerio de Ciencia, Tecnología e Innovación Productiva (Argentina). This work was in part supported by the ANR COSMISME project, grant ANR-2010-BLAN-0502 of the French Agence Nationale de la Recherche. G.M.M.C. was supported by project AYA2008-06374 funded by Spanish MICINN.

References

Adamson, A. J., Whittet, D. C. B., & Duley, W. W. 1990, MNRAS, 243, 400
Allamandola, L. J., Sandford, S. A., Tielens, A. G. G. M., & Herbst, T. M. 1993, Science, 260, 64
Araya, E., Hofner, P., Linz, H., et al. 2004, ApJS, 154, 579
Araya, E., Hofner, P., Goss, W. M., et al. 2007, ApJS, 170, 152
Balachandran, S. 1990, ApJ, 354, 310
Bessell, M. S., & Brett, J. M. 1988, PASP, 100, 1134
Boesgaard, A. M., & Tripicco, M. J. 1986, ApJ, 303, 724
Bottinelli, S., Adwin Boogert, A. C., Bouwman, J., et al. 2010, ApJ, 718, 1100
Brand, J., & Blitz, L. 1993, A&A, 275, 67
Bridger, A., Wright, G. S., & Geballe, T. R. 1994, in Infrared Astronomy with Arrays: The Next Generation, ed. I. S. McLean, Astrophysics and Space Science Library, 190, 537
Brooke, T. Y., Sellgren, K., & Geballe, T. R. 1999, ApJ, 517, 883
Chiar, J. E., & Tielens, A. G. G. M. 2001, ApJ, 550, L207
Chiar, J. E., Adamson, A. J., & Whittet, D. C. B. 1996, ApJ, 472, 665
Chiar, J. E., Tielens, A. G. G. M., Whittet, D. C. B., et al. 2000, ApJ, 537, 749
Chiar, J. E., Adamson, A. J., Pendleton, Y. J., et al. 2002, ApJ, 570, 198
Cotera, A. S., Simpson, J. P., Erickson, E. F., et al. 2000, ApJS, 129, 123
Cutri, R. M., Skrutskie, M. F., van Dyk, S., et al. 2003, 2MASS All Sky Catalog of point sources., ed. R. M. Cutri, M. F. Skrutskie, S. van Dyk, et al. (NASA/IPAC Infrared Science Archive)
Dartois, E., & d'Hendecourt, L. 2001, A&A, 365, 144
Dartois, E., & Muñoz-Caro, G. M. 2007, A&A, 476, 1235
Dartois, E., d'Hendecourt, L., Thi, W., Pontoppidan, K. M., & van Dishoeck, E. F. 2002, A&A, 394, 1057
Dartois, E., Marco, O., Muñoz-Caro, G. M., et al. 2004, A&A, 423, 549
Faustini, F., Molinari, S., Testi, L., & Brand, J. 2009, A&A, 503, 801
Fontani, F., Cesaroni, R., & Furuya, R. S. 2010, A&A, 517, A56
Gosling, A. J., Bandyopadhyay, R. M., & Blundell, K. M. 2009, MNRAS, 394, 2247
Hodapp, K. W., Jensen, J. B., Irwin, E. M., et al. 2003, PASP, 115, 1388
Imanishi, M. 2000a, MNRAS, 313, 165
Imanishi, M. 2000b, MNRAS, 319, 331
Imanishi, M., Sasaki, Y., Goto, M., et al. 1996, AJ, 112, 235
Ishii, M., Nagata, T., Sato, S., et al. 1998, AJ, 116, 868
Ishii, M., Nagata, T., Chrysostomou, A., & Hough, J. H. 2002, AJ, 124, 2790
Kurtz, S., Hofner, P., & Álvarez, C. V. 2004, ApJS, 155, 149
McFadzean, A. D., Whittet, D. C. B., Bode, M. F., Adamson, A. J., & Longmore, A. J. 1989, MNRAS, 241, 873
Mennella, V. 2010, ApJ, 718, 867
Molinari, S., Brand, J., Cesaroni, R., & Palla, F. 1996, A&A, 308, 573
Nishiyama, S., Nagata, T., Tamura, M., et al. 2008, ApJ, 680, 1174
Pandian, J. D., Goldsmith, P. F., & Deshpande, A. A. 2007, ApJ, 656, 255
Pendleton, Y. J., Sandford, S. A., Allamandola, L. J., Tielens, A. G. G. M., & Sellgren, K. 1994, ApJ, 437, 683
Rawlings, M. G., Adamson, A. J., & Whittet, D. C. B. 2003, MNRAS, 341, 1121
Rieke, G. H., & Lebofsky, M. J. 1985, ApJ, 288, 618
Rieke, G. H., Rieke, M. J., & Paul, A. E. 1989, ApJ, 336, 752
Sandford, S. A., Allamandola, L. J., Tielens, A. G. G. M., et al. 1991, ApJ, 371, 607
Sandford, S. A., Pendleton, Y. J., & Allamandola, L. J. 1995, ApJ, 440, 697
Schödel, R., Najarro, F., Muzic, K., & Eckart, A. 2010, A&A, 511, A18
Soifer, B. T., Russell, R. W., & Merrill, K. M. 1976, ApJ, 207, L83
Spoon, H. W. W., Armus, L., Cami, J., et al. 2004, ApJS, 154, 184
Tokunaga, A. T. 2000, Infrared Astronomy, 4th ed., ed. Cox, A. N. (New York: AIP Press; Springer), 143
Vig, S., Testi, L., Walmsley, M., et al. 2007, A&A, 470, 977
Watt, S., & Mundy, L. G. 1999, ApJS, 125, 143
Whittet, D. C. B. 1992, Dust in the galactic environment (Institute of Physics Publishing)
Whittet, D. C. B., Boogert, A. C. A., Gerakines, P. A., et al. 1997, ApJ, 490, 729
Wickramasinghe, D. T., & Allen, D. A. 1980, Nature, 287, 518